Supplementary Materials

Table S1. Thermoanalytical data for nickel based catalysts.

Catalyst	Σ weight loss, %
$NiMg_4Al_2$-HT	39.2
$Ni_{1.3}Mg_{3.7}Al_2$-HT	39.5
$Ni_{1.6}Mg_{3.4}Al_2$-HT	39.9
$Ni_2Mg_3Al_2$-HT	41.6

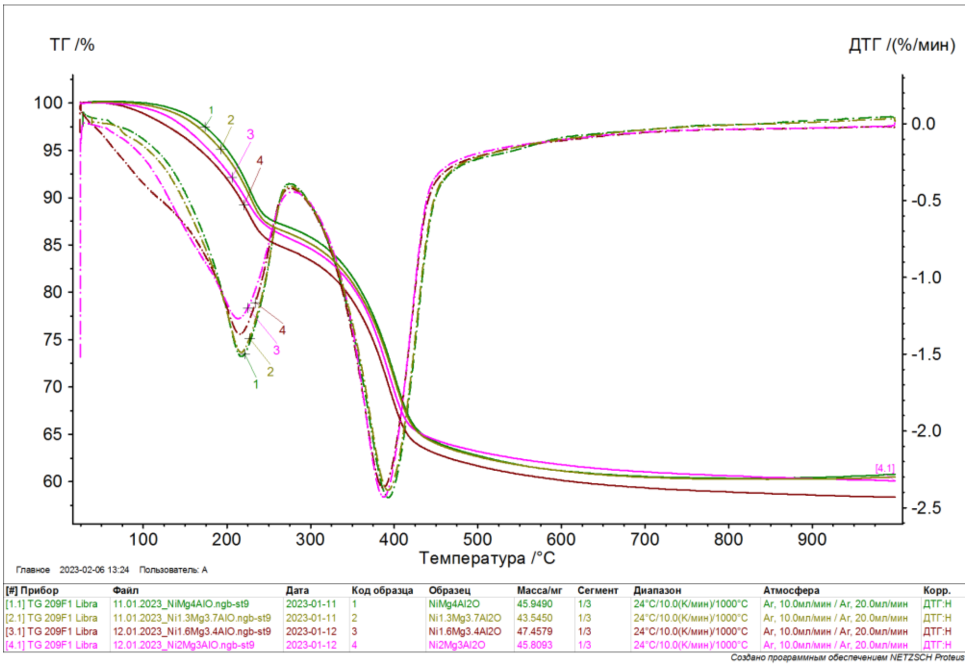

Figure S1. DTA and DTG profile of the samples.

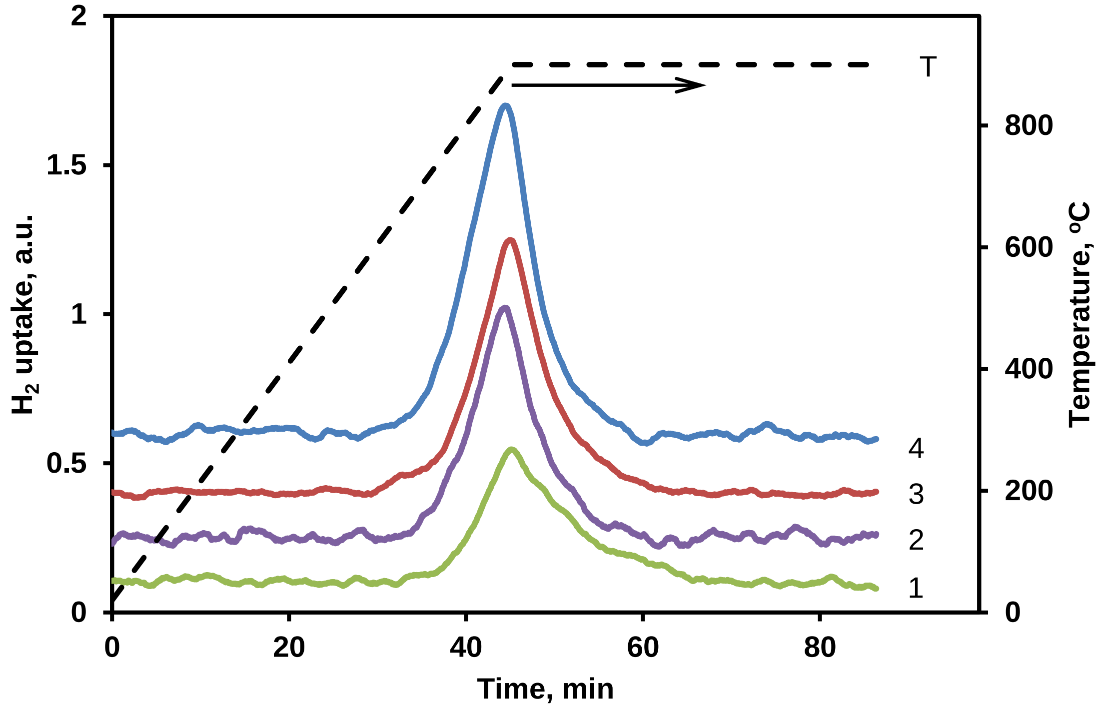

Figure S2. Time dependence of H_2 MS-signal and temperature for $Ni_xMg_yAl_2$-HT samples calcined at 600˚C (1- $NiMg_4Al_2$-HT, 2 - $Ni_{1.3}Mg_{3.7}Al_2$-HT, 3 - $Ni_{1.6}Mg_{3.4}Al_2$-HT, 4 - $Ni_2Mg_3Al_2$-HT).

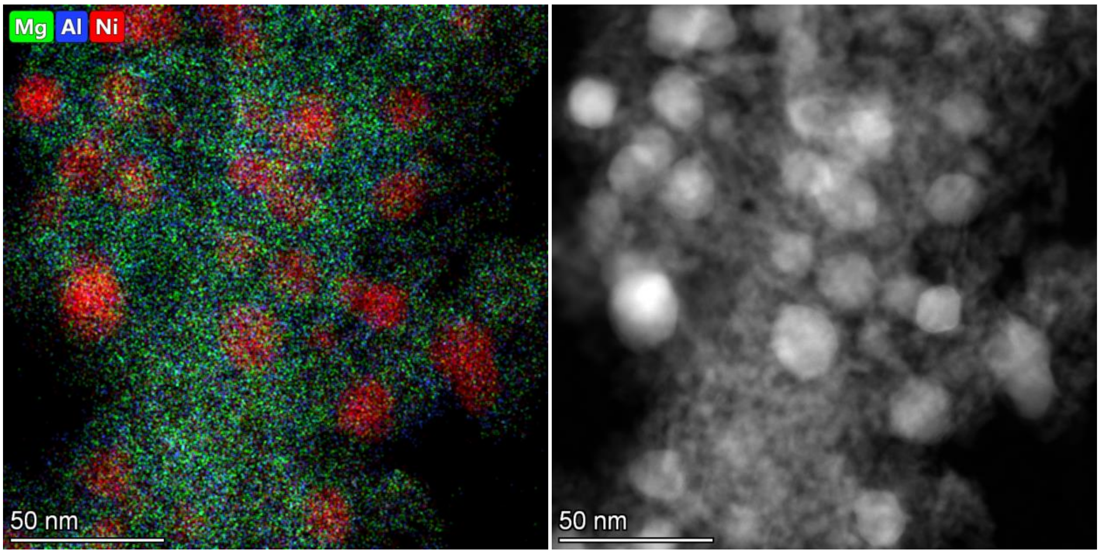

Figure S3. HAADF STEM (left) and EDX elemental mapping (right) of reduced $Ni_2Mg_3Al_2$-HT sample (700˚C, H_2).

Table S2. Comparison of the ammonia decomposition activity of nickel based catalysts.

Catalyst	Ni content wt.%	GHSV, ml/ (g_{cat}•h)	NH_3 inlet flow, %	T,°C	Conversion, %	H_2 rate, mmol/ (g_{cat}•min)	E_a, kJ/mol	Ref.
Ni/Al_2O_3	40.5	30000	100	500	31	10.4	-	[1]

Ni/$Mg_{0.29}Al_{0.57}O_n$	40.1	30000	100	500	42	14.1	-	[1]
Ni/La-MgO	20	22000	100	500	84	21.0	182	[2]
Ni/$BaZrO_3$	40	6000	100	500	67	4.5	-	[3]
Ni/$SrZrO_3$	40	6000	100	500	61	4.1	-	[3]
Ni/ $CaZrO_3$	40	6000	100	500	23	1.5	-	[3]
Ni/ZrO_2	40	6000	100	500	10.5	0.7	-	[3]
Ni/$BaTiO_3$	40	6000	100	500	34	2.3	-	[3]
Ni/$SrTiO_3$	40	6000	100	500	42	2.8	-	[3]
Ni/$CaTiO_3$	40	6000	100	500	15	1.0	-	[3]
Ni/TiO_2	40	6000	100	500	12	0.8	-	[3]
Ni/MCF-17		6000	100	500	40	2.7	-	[4]
Ni/sepiolite	20	2000	100	500	82	1.8	105	[5]
Ni/Al_2O_3	20	7500	100	500	27.2	2.0	-	[6]
Ni/Ce-Al_2O_3	20	7500	100	500	53	4.4	41	[7]
Ni/Zr-Al_2O_3	20	7500	100	500	49	4.1	42	[7]
Ni/Al_2O_3	8.9	9000	100	500	27	2.7	92	[8]
Ni/Al-$Ce_{0.8}Zr_{0.2}O_2$	8	9000	100	500	58	5.8	67	[8]
Ni/hydrocalumite	23.6	30000	100	500	20.4	6.8	-	[9]
Ni/Ni_MgAl(6:1)	15	60000	100	500	17	11.4	-	[9]
Ni/ZSM-5	5	30000	100	500	42	14.1	-	[9]

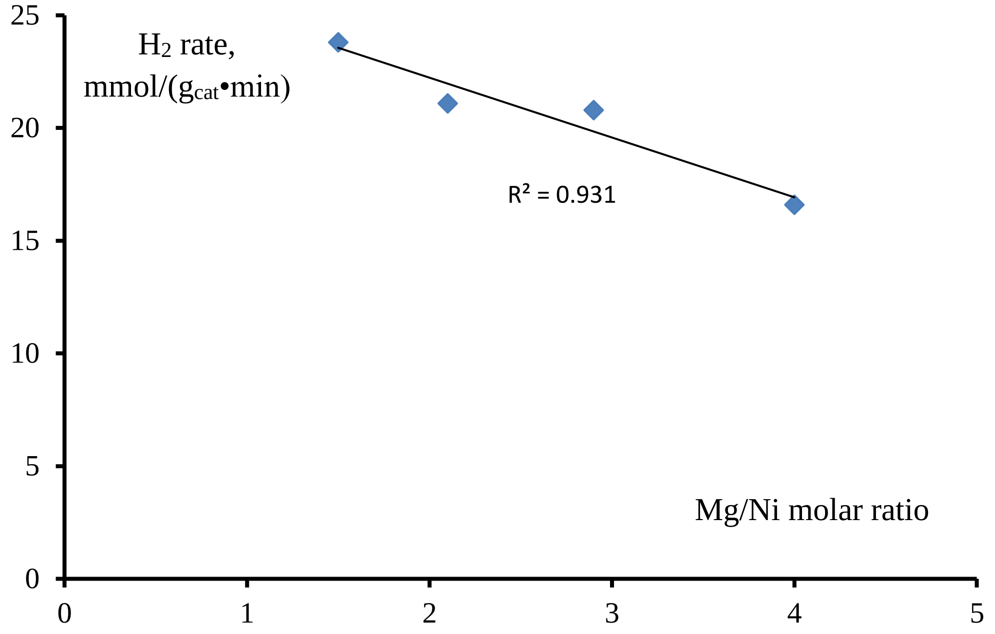

Figure S4. Correlation between the Mg/Ni molar ratio and the H_2 formation rates (mmol $H_2/(g_{cat}$•min) for NH_3 conversion over $Ni_xMg_yAl_2$-HT catalysts (700˚C, H_2) (flow rate 60 mL/min).

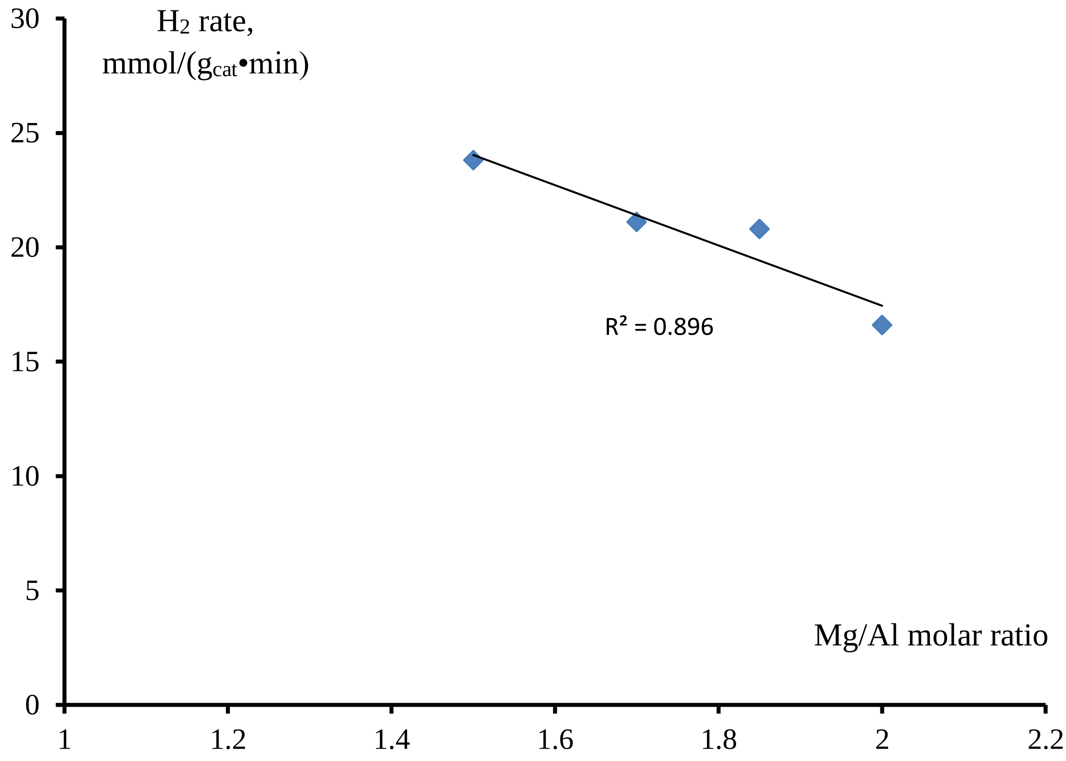

Figure S5. Correlation between the Mg/Al molar ratio and the H_2 formation rates (mmol $H_2/(g_{cat}$•min) for NH_3 conversion over $Ni_xMg_yAl_2$-HT catalysts (700˚C, H_2) (flow rate 60 mL/min).

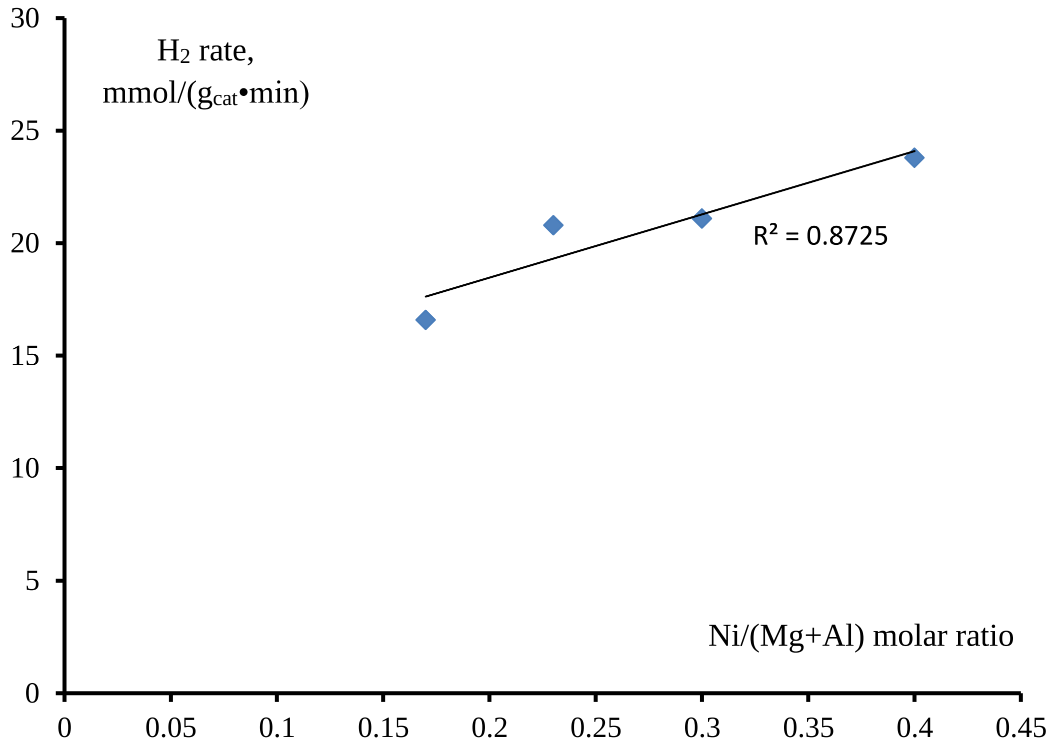

Figure S6. Correlation between the Ni/(Mg+Al) molar ratio and the H_2 formation rates (mmol H_2/(g_{cat}•min) for NH_3 conversion over $Ni_xMg_yAl_2$-HT catalysts (700˚C, H_2) (flow rate 60 mL/min).

References

S1 Hu X.-C., Wang W.-W., Jin Z., Wang X., Si R., Jia C.-J. Transition metal nanoparticles supported La-promoted MgO as catalysts for hydrogen production via catalytic decomposition of ammonia, J. En.Chem. **2019**, 38, 41–49. https://doi.org/10.1016/j.jechem.2018.12.024.

S2 Okura K., Miyazaki K., Muroyama H., Matsui T., Eguchi K. Ammonia decomposition over Ni catalysts supported on perovskite-type oxides for the on-site generation of hydrogen. RSC Adv. **2018**, 8, 32102–32110. https://doi.org/10.1039/C8RA06100A.

S3 Li Y., Wen J., Ali A.M., Duan M., Zhu W., Zhang H., Chen C., Li Y. Size structure–catalytic performance correlation of supported Ni/MCF-17 catalysts for CO_x -free hydrogen production. Chem. Commun. **2018**, 54, 6364–6367. https://doi.org/10.1039/C8CC01884G.

S4 Kurtoğlu S.F., Sarp S., Yılmaz Akkaya C., Yağcı B., Motallebzadeh A., Soyer-

Uzun S., Uzun A. COx -free hydrogen production from ammonia decomposition over sepiolite-supported nickel catalysts. Int. J. Hydr. En. **2018**, 43, 9954–9968. https://doi.org/10.1016/j.ijhydene.2018.04.057.

S5 Henpraserttae S., Charojrochkul S., Klysubun W., Lawtrakul L., Toochinda P. Reduced Temperature Ammonia Decomposition Using Ni/Zr-Doped Al_2O_3 Catalyst. Catal. Lett. **2018**, 148, 1775–1783. https://doi.org/10.1007/s10562-018-2381-9.

S6 Henpraserttae S., Charojrochkul S., Lawtrakul L., Toochinda P., Ni-based Catalysts for Hydrogen Production from Ammonia Decomposition: Effect of Dopants and Urine Application. Chem. Select. **2018**, 3, 11842–11850. https://doi.org/10.1002/slct.201802975.

S7 Sima D., Wu H., Tian K., Xie S., Foo J.J., Li S., Wang D., Ye Y., Zheng Z., Liu Y.-Q. Enhanced low temperature catalytic activity of Ni/Al–$Ce_{0.8}Zr_{0.2}O_2$ for hydrogen production from ammonia decomposition, Int. J. Hydr. En. **2020**, 45, 9342–9352. https://doi.org/10.1016/j.ijhydene.2020.01.209.

S8 Zhao J., Deng L., Zheng W., Xu S., Yu Q., Qiu X. Nickel-induced structure transformation in hydrocalumite for enhanced ammonia decomposition, Int. J. Hydr.En. **2020,** 45, 12244–12245. https://doi.org/10.1016/j.ijhydene.2020.02.201.

S9 Hu Z.-P., Weng C.-C., Chen C., Yuan Z.-Y. Catalytic decomposition of ammonia to COx-free hydrogen over Ni/ZSM-5 catalysts: A comparative study of the preparation methods. Appl. Catal. A Gen. **2018**, 562, 49–57. https://doi.org/10.1016/j.apcata.2018.05.038.